New Physics: Sae Mulli,
Vol. 67, No. 9, September 2017, pp. 1072∼1079
http://dx.doi.org/10.3938/NPSM.67.1072

Synthesis of a Sodium-Ion-Emitting Material and Analysis of Its Na^+ Emission Characteristics

Dae Sun Choi*
Department of Physics, Kangwon National University, Chunchon 24341, Korea

(Received 7 July 2017 : revised 25 July 2017 : accepted 25 July 2017)

In this study, I synthesized a β-eucryptite-like Na^+-emitting material for various purposes and analyzed quantitatively its emission characteristics. The results of a residual gas analysis showed that the purity of the emitted Na^+ ion was high and that the material had a very small amount of outgassing in an ultra-high vacuum, even at high temperatures. The maximum ion-beam current density was measured to be 18.2 A/m^2 when the filament potential was 1500 V and the filament temperature was 1270 K. The estimated ion-emitting energy was 3.36 eV, meaning that the Na^+ ion could be easily emitted. The measured half-life times for filament temperatures of 1270 K and 1190 K were 334.7 min and 2067.6 min, respectively, meaning that this material has a very long lifetime. I derived the ion-beam current density as a function of the filament temperature, filament potential, and working time. I conclude that these results can be applied to various industrial and research fields.

PACS numbers: 81.05.Zx
Keywords: Na^+, Ion, Synthesis, β-eucryptite-like material, Current density, Half-life times

I. INTRODUCTION

Many kind of ion sources [1–4] are widely used for industrial and research purposes, such as surface modification, doping in semiconductor and particle accelerator. However, most of ion sources have a complicated structure; therefore, it is difficult to construct them. The complicated structures are due to the complicated ion emitting (ionization) process. An ion emitter material of simple ionization process will be helpful to construct a simple ion source.

In the Low Energy Ion Scattering Spectroscopy (LEISS) [5–7] study, the detector detects particles scattered from the target surface to investigate the structure of the solid surface. The incident ion of the LEISS strongly affects the quality of the detected signals. Usually, He^+ ion is used in the LEISS study. The ionization energy of He^0 is much bigger than that of alkali atoms [8,9]. Therefore, the Auger neutralization probability of He^+ ion is bigger than that of alkali atoms. If the detector of the LEISS system is of the time of flight (TOF) type, it can detect neutral atoms as well as ions. However, if the detector is of the electrostatic analyzer (ESA) type, it cannot detect neutral atoms. Thus, alkali ion is more effective than He^+ ion in the ESA LEISS. Still, alkali elements are chemically active and, therefore, it is difficult to make alkali ion sources.

Besides ESA LEISS study, alkali ions are widely used in other applications. For example, alkali ions are used for ion implantation [10,11], as well as in doping [12,13], adsorption [14] and neutralization research [15–18].

Therefore, it is necessary to synthesize the alkali ion emitting material which has a simple emitting process and low neutralization probability for both the LEISS study and other applications.

In this study, I synthesized the thermionic emission type Na^+ ion emitting material based on the β-eucryptite [19] and analysed its emission characteristics. The ion emitting process of this solid state material is

*E-mail: dschoi@kangwon.ac.kr

very simple. Moreover, this synthesized Na^+ ion emitting material shows high purity, no outgassing in ultra-high vacuum, long half-life time, and high and long-time stability of ion beam current.

Overall, this synthesized ion emitting material can be used for doping study in semiconductors, ion implantation, and adsorption study as well as in the quality of the ion source for the LEISS study.

II. EXPERIMENT

It is known that when β-eucryptite ($Li_2O{\cdot}Al_2O_3{\cdot}2SiO_2$) is heated, Li atoms in this material acquire conductivity. This phenomenon is due to the dramatic thermal expansion coefficients of the bonding axis of this material. The thermal expansion coefficients of the crystallographic directions of this material α_a and α_c are $8.21 \times 10^{-6}/°C$ and $-17.6 \times 10^{-6}/°C$, respectively [20]. Li^+ ion can be emitted from crystal lattice due to this net effect of the anisotropic expansion. If Li^+ ion in β-eucryptite is substituted by an element in group I, that element also can be emitted from the crystal lattice, because that element has similar chemical properties as Li atom.

Sodium is the element in Group I and Li atoms in the β-eucryptite could be substituted by sodium atoms.

For the synthesis of the Na^+ ion emitting material, I mixed Na_2CO_3, $Al2O_3$ and SiO_2 powders uniformly with the molar ratios of 1, 1, and 2. Furthermore, I made this mixed powder into briquettes by compressing with the pressure of 1×10^4 N/cm^2. Briquette was heated up to 2100 K using tungsten filament in the vacuum chamber for several minutes. Usually, this process is performed in the He atmosphere furnace. Even in He atmosphere, it can be contaminated by a very small amount of oxygen, nitrogen, or other gases. So, I used the vacuum chamber to get the high purity ion source. This process is shown in Eq. (1).

$$\begin{aligned} &Na_2CO_3 + Al_2O_3 + 2SiO_2 \\ &\rightarrow Na_2O \cdot Al2O_3 \cdot 2SiO_2 + CO_2 \end{aligned} \qquad (1)$$

To investigate the emission characteristics of the β-eucryptite–like Na^+ ion emitting material ($Na_2O{\cdot}Al2O_3{\cdot}2SiO_2$: thereafter referred to as Na^+ ion emitting material or specimen), I grounded this material into very fine powder to enlarge the surface area of the material and painted it on the tungsten filament. The dimension of the spiral tungsten filament was 0.7 mm in diameter and 5 mm in length.

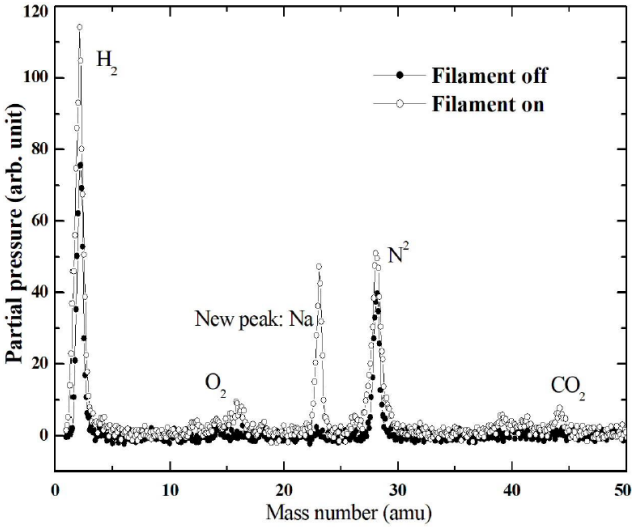

Fig. 1. RGA spectra. (1) Closed circles: before filament heating; (2) Open circles: when filament heating. The filament temperature is 1270 K and the filament potential is 100 volt.

The tungsten filament painted with specimen was inserted in the vacuum chamber with the base pressure of 1.3×10^{-7} Pa. To measure the emission current, I placed a copper plate in front of the filament. The distance between the filament and the plate was 5 mm. Most of the emitted Na^+ ions shall adsorb on the plate surface and small number of Na^+ ion shall be scattered from the plate surface and diffused in to the vacuum. A residual gas analyzer (RGA) placed near the filament was used to measure the impurity elements emitted from the specimen, as well as the scattered Na^+ ion and Na atoms.

III. RESULTS AND ANALYSIS

1. RGA results

Fig. 1 shows the RGA spectra. The closed circles denote the data points when the filament was not heated. It shows a strong H_2 peak and N_2 peak. However, when the filament was heated and positive potential with respect to the plate was applied to the filament, the RGA spectra (open circles) show small increments of H_2, N_2

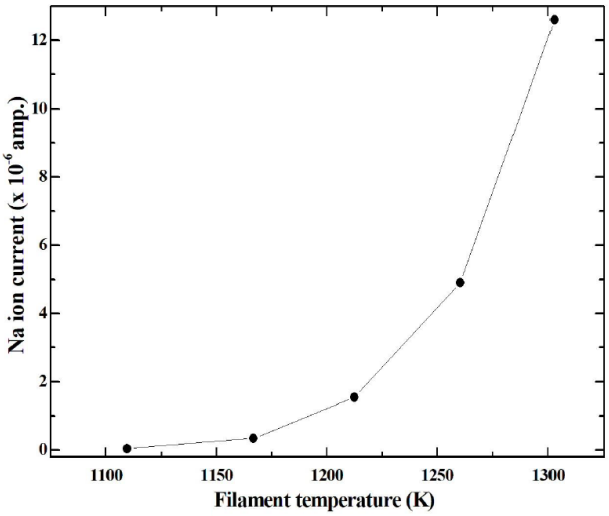

Fig. 2. The Na^+ ion beam current versus filament temperature. The filament potential is fixed at 100 volt.

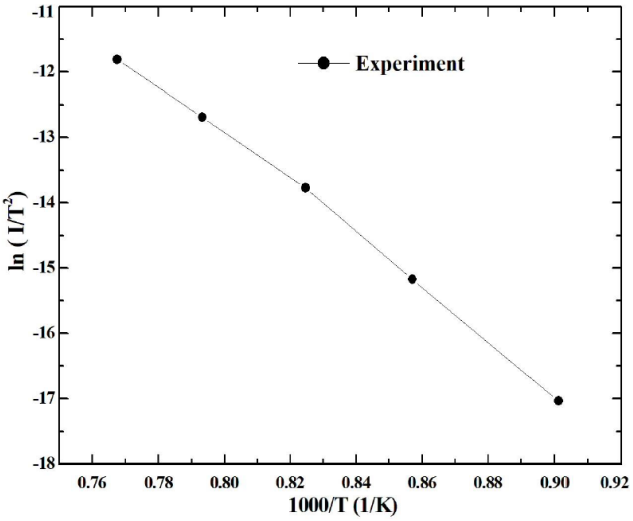

Fig. 3. The plot of $\ln(I/T^2)$ versus $1000/T$ when the filament potential is fixed at 100 volt.

peaks, very small increments of O_2, CO_2 peaks, and a new strong Na peak. Some of these increments may have been induced by desorbing phenomena from surroundings due to the thermal radiation from hot filament and some of these increments directly from hot specimen. However, the comparison of these two spectra results in the high purity of the emitted Na^+ ion. These spectra show that the Na^+ ion emitted from specimen when the positive potential was applied to the specimen and heated. The RGA detect only the scattered Na^+ ions and Na atoms. But some of scattered Na^+ ions or Na atoms can adsorb on the wall of the vacuum chamber before they arrive at the RGA detector. The distance between the RGA head and the filament is ∼5 cm. If the distance is shorter, the Na peak should be stronger because chemically active Na^+ ions or Na atoms have a bigger probability to arrive to the RGA detector without adsorbing on the wall of vacuum chamber.

2. Effect of filament temperature on the Na ion emission current

It is well known that the resistance of material varies with its temperature. I measured the filament temperature by measuring the resistance of the filament. I estimated the resistance of the filament by measuring the filament current and the filament voltage.

It is known that the emission current from hot cathode is given by following Richardson equation [21] (see Eq. (2)):

$$J = AT^2 e^{\frac{-E}{kT}}, \tag{2}$$

where A is a constant given by the physical or chemical properties of the emitter, E is barrier height, and k is the Boltzmann constant. Note, in the case of electron emission, E is the work function of the emitter material. Although Eq. (2) is derived to explain the electron emission from the solid, it is still available to ions because when they derived Eq. (2), they did not distinguish electron from positive ion.

Fig. 2 shows the Na ion beam current versus filament temperature. The filament potential is fixed at 100 volt. To measure energy E, it is convenient to use the following logarithmic plot (see Eq. (3)):

$$\ln\left(\frac{J}{T^2}\right) = \ln A - \frac{E}{kT} \tag{3}$$

Fig. 3 shows the plot $\ln\left(\frac{I}{T^2}\right)$ versus 1000/T. The slope of this plot is -E/(1000 k) and the energy E is determined to be 3.36 ± 0.05 eV. W and LaB_6 are used for a good electron source. The work function of W is 4.5∼5.3 eV [22,23] and LaB_6 is 2.4∼2.7 eV [24]. If I compare this result of 3.36 eV with the work functions of W and LaB_6, I can conclude that this synthesized material is a good Na^+ ion source.

3. Effect of filament potential on the Na^+ ion emission current

The emission current density also depends on the filament potential with the respect to the plate. There are two effects of the filament potential on the current density. The one is the velocity of ion obtained by the acceleration due to the potential difference $V(x)$ between the filament and the plate, while the other is the field effect. The field effect will be explained later. The Child-Langmuir model [25–27] can explain the relation between current density and applied potential. The authors show that the current density J is proportional to the $V^{2/3}$ where V is the potential difference between the cathode and the anode. The authors derived their equation using the parallel plate model (plane cathode and plane anode). Therefore, their model cannot explain this cylindrical system; furthermore, their model is valid only for parallel plates system. To get the relation between current density J and the filament potential V in this system, we should solve the Poisson' s equation in the cylindrical coordinate. The Poisson' s equation is given by the following (see Eq. (4)):

$$\nabla^2 V = -\frac{\rho}{\varepsilon_0} \tag{4}$$

The charge density ρ varies with r, where r is the distance from the emitter to observation point. To solve this equation, one should express the charge density ρ as a function of current density J. If one set ne to be ρ, where n is the number of ions per unit volume and e is the electron charge unit, the current density J is $-nev$, where v is the velocity of the ion near the plate and the negative sign means that the observation point has a negative potential with respect to the ion emitter. Then, ρ is given by $-J/v$. If one set ρ as $+J/v$, the V in Eq. (4) should be replaced by $-V$.

The velocity of a single charged ion accelerated from filament to anode by the potential difference $V(v)$ is given by Eq. (5).

$$v(r) = \sqrt{\frac{2eV(r)}{m}}, \tag{5}$$

then space charge density ρ is as follows (see Eq. (6)):

$$\rho = -J\sqrt{\frac{m}{2eV(r)}}. \tag{6}$$

Than the Poisson' s equation is given by the following (see Eq. (7)):

$$\nabla^2 V = B\frac{1}{\sqrt{V(r)}}, \tag{7}$$

where B is $\sqrt{\frac{m}{2e\varepsilon_0^2}}$. The Poisson' s equation in cylindrical coordinate is as follows (see Eq. (8)):

$$\frac{1}{r}\frac{\partial}{\partial r}\left(r\frac{\partial}{\partial r}V\right) = B\frac{J}{\sqrt{V(r)}}. \tag{8}$$

One can set the potential as follows (see Eq. (9)):

$$V(r) = \alpha r^n + \beta. \tag{9}$$

Here, α and β are the constants and it is not necessary for n to be integer number. If one set r_0 to be the radius of cylinder (filament), using the initial condition $V(r_0)$ = 0 volt, one can get $\beta = -\alpha r_0^n$.

Substituting this $V(r)$ in Eq. (8) yields the following equation (see Eq. (10)):

$$\alpha n^2 r^{n-2} = BJ\alpha^{-1/2} r^{-n/2}\left(1 - \frac{r_0}{r}\right)^{-n/2} \tag{10}$$

From Eq. (10), one can numerically determine α and n. In most cases, the radius of the filament r_0 is much shorter than the distance between filament and plate and one can ignore $\frac{r_0}{r}$ in Eq. (10). If one ignore $\frac{r_0}{r}$, n is 4/3 and α is $\left(\frac{9BJ}{16}\right)^{2/3}$. Substituting α and n in Eq. (9) yields the potential (see Eq. (11)),

$$V(r) \approx \left(\frac{9BJ}{16}\right)^{2/3} r^{4/3}. \tag{11}$$

If the distance between the filament and the plate is D and the potential difference between the filament and the anode is V_0, the relation between D and V_0 is as follows (see Eq. (12)):

$$V_0 \approx \left(\frac{9BJ}{16}\right)^{2/3} D^{4/3}. \tag{12}$$

Rearrangement of Eq. (12) yields the current density in the cylindrical coordinate J_{cy} as follows (see Eq. (13)):

$$J_{cy} \approx \left(\frac{16\varepsilon_0}{9D^2}\right)\left(\frac{2e}{m}\right)^{1/2} V_0^{3/2} \tag{13}$$

If one solve the Poisson' s equation in the spherical coordinate and in the rectangular coordinate, the current densities J_{sp} and J_{re} are as follows (see Eqs. (14)-(15)):

$$J_{sp} = \left(\frac{28\epsilon_0}{9D^2}\right)\left(\frac{2e}{m}\right)^{1/2} V_0^{3/2}, \tag{14}$$

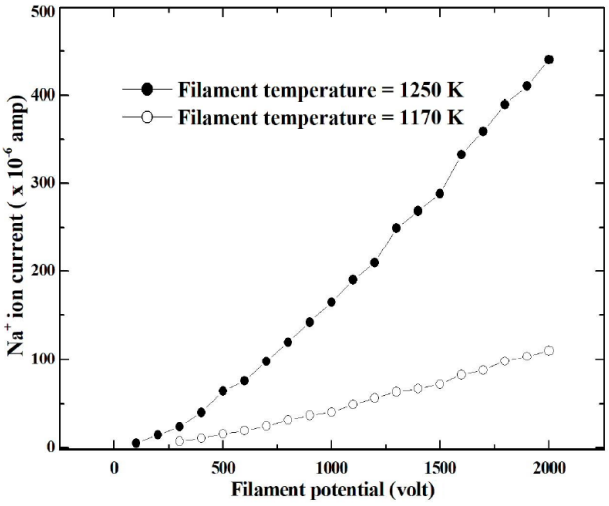

Fig. 4. Plots of Na^+ ion current versus filament potential when the filament temperatures are 1170 K (open circle) and 1250 K (closed circle).

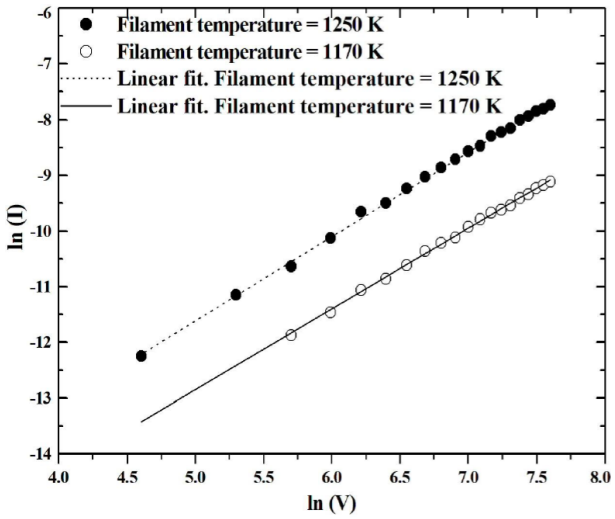

Fig. 5. Plots of $\ln(I)$ versus $\ln(V)$. The graph shows straight lines. The slopes of these lines are 1.51 at the filament 1250 K and 1.45 at 1170 K, respectively.

and

$$J_{re} = \left(\frac{4\epsilon_0}{9D^2}\right)\left(\frac{2e}{m}\right)^{1/2} V_0^{3/2}, \tag{15}$$

respectively.

In most cases, the shape of the filament (cathode) and the anode are not parallel plates, not concentric spheres or concentric cylinders. Therefore, Eqs. (13) – (15) should be modified according to the proper boundary conditions. The equation of spherical coordinate Eq. (14) may be useful for the pin point ion or electron emitting source.

However, it is clear that the current densities are proportional to $V_0^{3/2}$ in any case.

Fig. 4 shows the plots of Na^+ ion current versus filament potential when the filament temperatures are 1170 K and 1250 K. This figure does not show the detailed exponent of V_0 in Eq. (13). The logarithmic plots are helpful to get the detailed exponent *i.e.* (see Eq. (16)).

$$\ln J = \ln \eta + \frac{3}{2}\ln V_0, \tag{16}$$

where $\ln\eta$ is a proportional constant that depends on the shapes of the filament and the anode.

Fig. 5 shows the plots of $\ln(I)$ versus $\ln(V)$. The graph shows straight lines. The slopes of these lines are 1.51 at the filament 1250 K and 1.45 at 1170 K, respectively. These values are in good agreement with Eq. (16).

If the strong electric field is applied to the filament, the electrons or ions can be emitted from solid to the vacuum by the tunneling effect. This effect is called field emission [28].

In the case of the electron, the barrier height is called work function and a simple calculation using uncertainty principle shows that the electric field needed an electron to emit from solid to vacuum is given by following equation (see Eq. (17)):

$$F_e = \sqrt{2me}\varphi^{3/2}\hbar, \tag{17}$$

where F_e is the electric filed, e is the electron charge unit, φ is the barrier height (in the case of electron, it is work function) in the unit of joule. If one applied this equation to the electron, the electric field to emit the electron is $\sim 10^9$ v/m. In the case of ion, the mass of ion is much heavier than electron and it needs a much stronger electric field to emit ion from solid to vacuum. Therefore, one may ignore the field emission effect on the ion beam current.

Finally, one can find the emission current as the function of filament temperature T and filament potential V. The current density equation is given by Eq. (18).

$$J = CT^2 e^{-E/kT} V^{3/2}. \tag{18}$$

Of note, $\ln\eta$ in Eq. (16) is $\ln\left(CT^2e^{-E/kT}\right)$ and $\ln A$ in Eq. (3) is $\ln\left(CV^{3/2}\right)$.

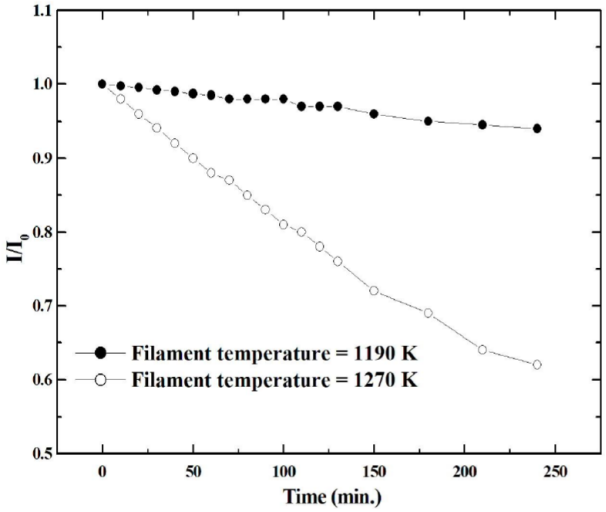

Fig. 6. Normalized ion current versus time. The filament potential is fixed at 1500 volt with respect plate.

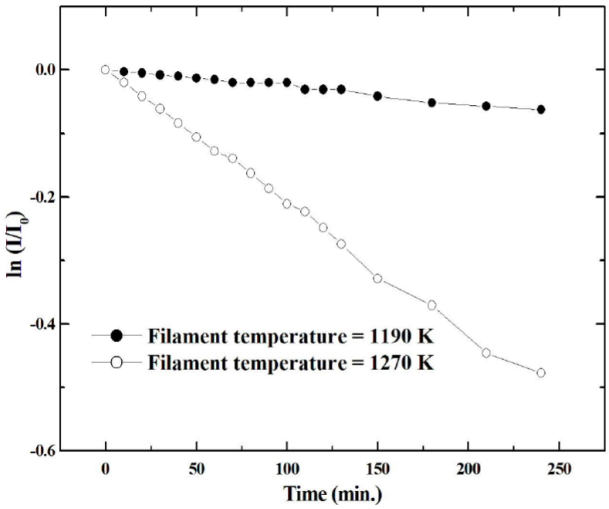

Fig. 7. The plot of $\ln\left(\frac{I}{I_0}\right)$ versus time.

4. Time dependence of the ion current density and the life time of the ion emitting material

The number of Na atoms in the specimen is finite. When Na^+ ions are emitted from the specimen, the total number of Na atoms decrease and this decrement results in reducing of emitting current density. If the total number of Na^+ ion in the specimen is n and $\frac{dn}{dt}$ is the number of ions emitted per unit time, $\frac{dn}{dt}$ is proportional to the total number n, *i.e.*, as shown in Eq. (19),

$$\frac{dn}{dt} = -\gamma n, \tag{19}$$

where γ is decay constant and the negative sign means the decrement of total number of n. The solution of this differential equation is a follows (see Eq. (20)):

$$n = n_0 e^{-\gamma t}\ , \quad \frac{dn}{dt} = -\gamma n_0 e^{-\gamma t}, \tag{20}$$

where n_0 is the initial total number of ions in the emitter. The current density J is proportional to $\frac{dn}{dt}$ and the decrement of n in the source material means the increment of emitted ion current. Therefore, the current density J is given by Eq. (21).

$$J = D\gamma n_0 e^{-\gamma t}, \tag{21}$$

where D is constant. At $t = 0$, $D\gamma n_0$ in Eq. (21) should be equal to $CT^2 e^{-E/kT} V^{3/2}$ that appeared in Eq. (18), *i.e.*, γ is proportional to $T^2 e^{-E/kT} V^{3/2}$. Therefore, the time, temperature, and potential dependent emission current density are given by Eq. (22).

$$J = CT^2 e^{-E/kT} V^{3/2} e^{-\gamma t}. \tag{22}$$

5. Half-life time

If one define the time constant as shown in Eq. (23).

$$\tau = 1/\gamma, \tag{23}$$

the half-life time t_h is given by Eq. (24).

$$t_h = \tau \ln 2 = \ln 2/(\xi T^2 e^{-E/kT} V^{3/2}), \tag{24}$$

where ξ is a proportional constant determined by the surface area of emitter and initial total number of ions in the in the emitter.

Fig. 6 shows the normalized ion current versus time. The filament potential is fixed at 1500 volt. When the filament temperature is 1190 K (closed circles), it decays very slow and decreases only by 5% during 250 minutes. However, when the filament temperature is 1270 K, it decays fast. Fig. 7 shows the plot of $\ln\left(\frac{I}{I_0}\right)$ versus time. The estimated half-life times for the filament temperatures 1270 K and 1190 K using the slopes of lines in Fig. 7 are 334.7 min. and 2067.6 min, respectively. The ratio $t_{h,1190K}/t_{h,1270K}$ is 7.79.

Fig. 8 shows the calculated half-life time versus filament temperature. This figure shows that, when the filament temperature is low, the half-life time is very long. The calculated $t_{h,1190K}/t_{h,1270K}$ using this figure is 8.06. Although there is a small difference between experimental results and the theoretically predicted value, these experimental results are in a good agreement with the theoretical value.

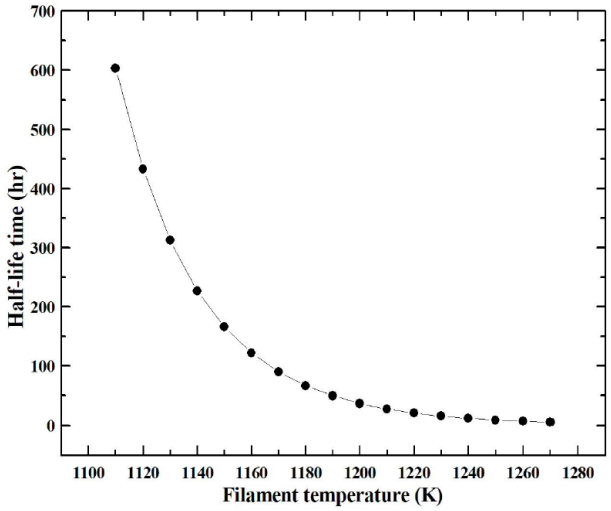

Fig. 8. Half-life time of Na^+ ion emitting material ($Na_2O{\cdot}Al_2O_3{\cdot}2SiO_2$). The filament potential is 1500 volt.

6. Maximum current density and stability of Na^+ ion beam

When the filament current was 1270 K and the filament potential was 1500 volt, initial Na^+ ion current was 200 μA (current density: 18.2 A/m^2) and when the filament temperature was 1190 K and the filament potential was 1500 volt, the initial beam current was 27 μA (2.45 A/m^2) and decreased by only 5% during 250 minutes. The fluctuations of the beam currents were below 0.5% at both of temperatures. Therefore, although the ion beam current depends on the surface area of the emitter, I can conclude that these ion beam currents are high enough to use in LEISS study and in the other applications.

As shown in Fig. 8, when the filament temperature is low, the half-life time is very long. This long half-life time means that this synthesized specimen is a good Na^+ ion emitting material. Together with adjusting the size of the emitter and using the half-life time data shown in Fig. 8, one can determine the ion beam current and the life time of the Na^+ ion source for various purposes.

IV. CONCLUSION

In this study, I have synthesized Na^+ ion source material for the purpose of using in the filament type ion gun and for the various applications such as ion implantation, doping study, adsorption study and so on. When I painted it in the filament and heated the filament, the RGA results show a strong Na peak and no other peak except for a very small amount of increment of N_2, H_2, O_2 and CO_2 gases. The ion beam current density was measured to be 18.2 A/m^2 when filament potential was 1500 volt and filament temperature was maintained at 1270 K and 2.45 A/m^2 when filament temperature was 1190 K. These current densities are high enough to use this material in the LEISS study as well as in the other applications. The estimated ion emitting energy was 3.36 eV, meaning that Na^+ ion can be easily emitted. The ion beam current decreases rapidly when the filament temperature is increased, but it decreases only by 5% during 250 minutes when the filament temperature is 1170 K. If one set the filament temperature to be lower, one can get smaller decrement for longer working time. However, this specimen has a very long half-life time. The derived the ion current density function is very useful to determine the ion beam current and life time of the ion source material. Therefore, the synthesized Na^+ ion source has good outgassing characteristics, high purity, high ion current density, low ion emitting energy, very long half-life time, and good beam stability. Thus, I can conclude that these results provide meaningful implications for further research on ion source used in various fields, as well as will help construct a good Na^+ ion gun.

REFERENCES

[1] S. L. Koontz and M. B. Denton, Int. J. Mass Spectr. Ion Phys. **37**, 227 (1981).

[2] P. C. Selvin and T. Fujii, Rev. Sci. Instrum. **72**, 2248 (2001).

[3] G. E. Bugrov, S. K. Kondranin, E. A. Kralkina, V. B. Pavlov and D. V. Savinov *et al.*, Curr. Appl. Phys. **3**, 485 (2003).

[4] B. S. Cho, H. J. Oh, H. S. Uhm, S. O. Kang and C. Kim *et al.*, Curr. Appl. Phys. **11**, S172 (2011).

[5] H. H. Brongersma, M. Draxlerc, M. de Riddera and P. Bauerc, Surf. Sci. Rep. **62**, 63 (2007).

[6] D. S. Choi, M. Kopczyk, A. Kayani, R.J. Smith and G. Bozzolo, Phys. Rev. B **74**, 115407 (2006).

[7] D. S. Choi and D. H. Kim, Thin Solid Films **520**, 6012 (2012).
[8] D. Geobl, R. C. Moneral, D. Valdes, D. Primetzhofer and P. Bauer, Nucl. Instrum. Methods Phys. Res. B **269**, 1296 (2011).
[9] K. Niedfeldt, E. A. Cartera and P. Nordlander, J. Chem. Phys. **121**, 3751 (2004).
[10] S. J. Pearton, C. B. Vartuli, J. C. Zolper, C. Yuan and R. A. Stall, Appl. Phys. Lett. **67**, 1435 (1995).
[11] S. O. Kucheyeva, J. S. Williamsa and S. J. Peartonb, Mater. Sci. Eng. **33**, 51 (2001).
[12] X. Yu and S. Raaen, Appl. Surf. Sci. **270**, 364 (2013).
[13] C. A. Howard, M. P. M. Dean and F. Withers, Phys. Rev. B **84**, 241404(R) (2011).
[14] H. Daimon and S. Ino, Surf. Sci. **164**, 320 (1985).
[15] A. R. Canario, A. G. Borisov, J. P. Gauyacq and V. A. Esaulov, Phys. Rev. B **71**, 121401 (2005).
[16] C. E. Sosolik, J. R. Hampton, A. C. Lavery, B. H. Cooper and J. B. Marston, Phys. Rev. Lett. **90**, 013201 (2003).
[17] S. Wethekam, D. Vald'es, R. C. Monreal and H. Winter, Phys. Rev. B **78**, 033105 (2008).
[18] M. Richard-Viard, C. B'enazeth, P. Benoit-Cattin, P. Cafarelli and N. Nieuwjaer, Phys. Rev. B **76**, 045432 (2007).
[19] C. A. Howard, M. P. M. Dean and F. Withers, Phys. Rev. B **84**, 241404(R) (2011).
[20] F. H. Gillery and E. A. Bush, J. Am. Ceram. Soc. **42**, 175 (1959).
[21] R. G. Lerner and G. L. Trigg, *Encyclopedia Physics*, 2nd ed. (Vch Publishers, Inc. New York, 1990), p. 1251.
[22] Y. Song and R. Gomer, Surf. Sci. **290**, 1 (1993).
[23] H. B. Michaelson, J. Appl. Phys. **48**, 4729 (1977).
[24] A. Yutani, A. Kobayashi and A. Kinbara, Appl. Surf. Sci. **70-71**, 737 (1993).
[25] M. S. Benilov, Plasma Sources Sci. Technol. **18**, 014005 (2009).
[26] C. D. Child, Phys. Rev. **32**, 492 (1911).
[27] I. Langmuir, Phys. Rev. **2**, 450 (1913).
[28] R. Gomer, *Field Emission and Field Ionization* (American Inst. of Phys., New York, 1961), p. 8.